BRAIN
A JOURNAL OF NEUROLOGY

Connexin-43 induces chemokine release from spinal cord astrocytes to maintain late-phase neuropathic pain in mice

Gang Chen,[1] Chul-Kyu Park,[1] Rou-Gang Xie,[1] Temugin Berta,[1] Maiken Nedergaard[2] and Ru-Rong Ji[1]

1 Departments of Anaesthesiology and Neurobiology, Duke University Medical Centre, Durham, NC, 27710, USA
2 Centre for Translational Neuromedicine, University of Rochester Medical Centre, Rochester, NY, 14642, USA

Correspondence to: Ru-Rong Ji, PhD,
Department of Anaesthesiology,
Duke University Medical Centre,
Durham, North Carolina,
NC, 27710, USA
E-mail: ru-rong.ji@duke.edu

Accumulating evidence suggests that spinal cord astrocytes play an important role in neuropathic pain sensitization by releasing astrocytic mediators (e.g. cytokines, chemokines and growth factors). However, it remains unclear how astrocytes control the release of astrocytic mediators and sustain late-phase neuropathic pain. Astrocytic connexin-43 (now known as GJ1) has been implicated in gap junction and hemichannel communication of cytosolic contents through the glial syncytia and to the extracellular space, respectively. Connexin-43 also plays an essential role in facilitating the development of neuropathic pain, yet the mechanism for this contribution remains unknown. In this study, we investigated whether nerve injury could upregulate connexin-43 to sustain late-phase neuropathic pain by releasing chemokine from spinal astrocytes. Chronic constriction injury elicited a persistent upregulation of connexin-43 in spinal astrocytes for >3 weeks. Spinal (intrathecal) injection of carbenoxolone (a non-selective hemichannel blocker) and selective connexin-43 blockers (connexin-43 mimetic peptides [43]Gap26 and [37,43]Gap27), as well as astroglial toxin but not microglial inhibitors, given 3 weeks after nerve injury, effectively reduced mechanical allodynia, a cardinal feature of late-phase neuropathic pain. In cultured astrocytes, TNF-α elicited marked release of the chemokine CXCL1, and the release was blocked by carbenoxolone, Gap26/Gap27, and connexin-43 small interfering RNA. TNF-α also increased connexin-43 expression and hemichannel activity, but not gap junction communication in astrocyte cultures prepared from cortices and spinal cords. Spinal injection of TNF-α-activated astrocytes was sufficient to induce persistent mechanical allodynia, and this allodynia was suppressed by CXCL1 neutralization, CXCL1 receptor (CXCR2) antagonist, and pretreatment of astrocytes with connexin-43 small interfering RNA. Furthermore, nerve injury persistently increased excitatory synaptic transmission (spontaneous excitatory postsynaptic currents) in spinal lamina IIo nociceptive synapses in the late phase, and this increase was suppressed by carbenoxolone and Gap27, and recapitulated by CXCL1. Together, our findings demonstrate a novel mechanism of astrocytic connexin-43 to enhance spinal cord synaptic transmission and maintain neuropathic pain in the late-phase via releasing chemokines.

Keywords: carbenoxolone (CBX); CXCL1; CXCR2; hemichannels; neuro-glial interaction

Abbreviations: CBX = carbenoxolone; CCI = chronic constriction injury; Cx43 = connexin-43; EPSC = excitatory postsynaptic current; TNF-α = tumor necrosis factor-alpha

Introduction

Neuropathic pain is a major health concern that represents a considerable social and economic burden worldwide. Patients diagnosed with neuropathic pain (i.e. pain that arises due to damage or disease to the somatosensory nervous system) report more severe pain and experience greater functional and quality of life impairments than patients diagnosed with a non-neuropathic mechanism (Jensen et al., 2007; van Hecke et al., 2013). Effective treatment, however, is hampered by an incomplete understanding of neuropathic pain's pathogenesis (Costigan et al., 2009).

It is generally believed that neuropathic pain is an expression of neural plasticity in primary sensory neurons (peripheral sensitization) (Hucho and Levine, 2007; Basbaum et al., 2009; Gold and Gebhart, 2010) and CNS neurons, such as spinal cord dorsal horn neurons (central sensitization) (Ji et al., 2003; Kuner, 2010). However, a number of studies over the past decades have recognized the importance of glial cells in maintaining homeostasis in the CNS (Kimelberg and Nedergaard, 2010), whereas other studies have identified ways in which glial cells actively contribute to synaptic events (Nedergaard and Verkhratsky, 2012). Astrocytes are the most abundant type of glial cell in the CNS, and accumulating evidence suggests that in the spinal cord they play an important role in neuropathic pain development and maintenance through the release of astroglial mediators that increase the activity of spinal cord nociceptive neurons (Gao and Ji, 2010a; Chiang et al., 2012). After nerve injury or spinal cord injury, spinal cord astrocytes demonstrate long-lasting reactive changes, which are associated with the persistence of neuropathic pain (Zhang and De Koninck, 2006; Chen et al., 2012; Shi et al., 2012; Ji et al., 2013). Spinal astrocytes also undergo proliferation in the first week of nerve injury (Tsuda et al., 2011). In neuropathic pain conditions, astrocytes have been shown to produce proinflammatory cytokines (e.g. IL-1beta), proteases (e.g. MMP2) and growth factors (e.g. FGF2), which promote neuropathic pain (Guo et al., 2007; Kawasaki et al., 2008; Gao and Ji, 2010b). Spinal cord astrocytes also produce proinflammatory chemokines, such as CCL2 (previously known as MCP1), CCL7 (previously known as MCP3), and CXCL1 (keratinocyte-derived cytokine), that have been shown to maintain neuropathic pain (Gao et al., 2009; Imai et al., 2013; Zhang et al., 2013). However, little is known about the molecular mechanisms that control the release of chemokines from activated astrocytes. Moreover, previous studies of neuropathic pain maintenance have focused on early phases that occur in the first 2 weeks after injury (Kawasaki et al., 2008; Tsuda et al., 2011), the specific role of glial cells in maintaining late-phase neuropathic pain remains unclear.

Astrocytes in the adult CNS form interconnected networks coupled by gap junctions. The major structural components of gap junctions are connexins and the connexin 43 (Cx43, now known as GJ1) subunit is the principal connexin expressed by astrocytes (Bennett et al., 2012). After spinal cord injury (Chen et al., 2012) and nerve stimulation (Wu et al., 2011; Yoon et al., 2013) Cx43 expression is upregulated. Deletion of Cx43 has been shown to attenuate neuroinflammation and improve functional recovery after spinal cord injury (Cronin et al., 2008). Strikingly, spinal cord injury-induced neuropathic pain was abolished in Cx43/Cx30 double knockout mice, but not in Cx30 knockout mice, suggesting an essential role of Cx43 in the development of central neuropathic pain (Chen et al., 2012). However, the specific role of Cx43 in the maintenance of late-phase neuropathic pain is unclear. When unopposed by an adjoining hemichannel, Cx43 was shown to control the astrocytic release of small molecules such as ATP and glutamate to the extracellular space (Stout et al., 2002; Ye et al., 2003; Bennett et al., 2012). We therefore investigated whether Cx43 could sustain late-phase neuropathic pain through the release of astrocytic chemokines. We found a persistent upregulation of Cx43 in spinal cord astrocytes after nerve injury, which is critical for the maintenance of late-phase neuropathic pain 3 weeks after nerve injury. In particular, our data demonstrate that Cx43 is required for tumour necrosis factor-alpha (TNF-α) elicited CXCL1 release by astrocytes. Patch clamp recordings from lamina II neurons additionally confirmed that CXCL1 released from astrocytic Cx43 potentiated neuropathic pain by direct modulation of excitatory synaptic transmission in the spinal cord.

Materials and methods

Animals and surgery

CD1 mice, obtained from Charles River Laboratories, were used for the majority of experiments. Adult CD1 mice (male, 25–32 g) were used for behavioural studies. Neonatal CD1 mice (postnatal Day 0–2) were used for preparing primary cultures of astrocytes. For select experiments, adult Gfap-GFP mice and Cx3cr1-GFP mice, obtained from The Jackson Laboratory, were used. The numbers of mice used in different experiments were shown in Supplementary Table 1. A total of 418 mice were used for in vivo, ex vivo (spinal cord slices), and in vitro (astrocyte cultures) studies. Neuropathic pain was produced using the model of chronic constriction injury (CCI) of the sciatic nerve (Bennett and Xie, 1988). In brief, animals were anaesthetized with isoflurane, then the left sciatic nerve was exposed and three ligatures (7-0 prolene) were placed around the nerve proximal to the trifurcation with a distance of 1 mm between each ligature. The ligatures were loosely tied until a short flick of the ipsilateral hind limb was observed. Animals in the sham group received surgery identical to those described but without nerve ligation. All animal procedures performed in this study were approved by the Animal Care Committee of Duke University Medical Centre.

Primary astrocyte cultures

Primary cultures of astrocytes were prepared as described previously (Gao et al., 2009). In brief, astrocyte cultures were prepared from cerebral cortices of neonatal mice on postnatal Day 0–2 and cultured in a 75 cm^2 flask at a density of 2.5×10^5 cells/cm^2 in low-glucose Dulbecco's modified Eagle medium containing 10% foetal bovine serum. We also prepared some astrocyte cultures from spinal cords of neonatal mice. Approximately 3–4 cortices or 10 spinal cords were used to prepare 12 cultures in a plate. The medium was replaced twice a week. After reaching confluence (10–12 days), the cells were shaken and re-plated on poly-D-lysine-coated glass coverslips or six-well plates at 10^6 cells/cm^2. Astrocytes formed a confluent layer 2–3 days after replating. In some cultures, immunostaining of GFAP and FGFR4 (marker of fibroblast) was performed to confirm the identity of

astrocytes in spinal cord cultures. Before experiments, 0.15 mM dibutyryl cAMP (Sigma) was added for 48 h to induce differentiation (Gao et al., 2009).

Fluorescence-activated cell sorting

Adult *Gfap*-GFP mice were anaesthetized and perfused with sterile PBS. The spinal cord lumbar segments were immediately dissected from the vertebral column, then cut into small pieces and dissociated in 0.25% trypsin for 15 min at 37°C. Cell mixtures were then filtered through a cell strainer (40 μm, Becton Dickinson) and resuspended in cold sterile PBS containing 1% bovine serum albumin ($2–3 \times 10^6$ cells/ml) for fluorescence-activated cell sorting (FACS). Cells were sorted using BD FACSVantage Cell Sorting System (13 psi sheath pressure, Cell Quest software). GFP was excited by a 488 nm laser and emissions were collected by a 530/30 nm discrimination filter. The signals were manually compensated, and cells were sorted into cold PBS with 1% bovine serum albumin.

Drugs and administration

TNF-α and CXCL1 were obtained from R&D, carbenoxolone (CBX), probenecid, L-α-aminoadipate, and minocycline were purchased from Sigma. Cx43 mimetic peptides (^{43}Gap26 and ^{37,43}Gap27), scrambled control peptide (Gap27 scrambled) and PANX1 mimetic peptide (^{10}Panx1) were purchased from AnaSpec. D-JNKI-1 was kindly provided by Dr Christopher Bonny, University of Lausanne, Switzerland (Zhuang et al., 2006). We also purchased SB 203580 from Calbiochem, SB 225002 from Tocris, CXCL1 neutralizing antibody from Boster, and normal Rabbit IgG from Santa Cruz.

Cx43 small interfering RNA (CAAUUCCUCCUGCCGCAAU) and non-targeting small interfering RNA (GACUUCGCGGGACACAUGA) were synthesized by Thermo Scientific Dharmacon. Small interfering RNA was dissolved in RNase-free water at 1 μg/μl as stock solution and mixed with the transfection reagent polyethyleneimine (Fermentas) and normal saline before use. Specifically, 1 μg small interfering RNA was dissolved in 3.3 μl of polyethyleneimine and 66 μl of normal saline (Gao et al., 2010c).

For intrathecal injection, spinal cord puncture was made with a 30-gauge needle between the L5 and L6 level to deliver reagents (10 μl) or cells (30 000 cells in 10 μl PBS) to the CSF. Before injection, astrocytes were washed with 0.01 M PBS three times, centrifuged for 5 min at 3000g, and then resuspended in PBS.

Enzyme-linked immunosorbent assay

Mouse CCL2 and CXCL1 ELISA kits were purchased from R&D Systems. For primary cultures of astrocytes, culture medium and cells were collected separately after treatment. For astrocytes of adult mice, 30 000 astrocytes after cell sorting were used in each condition. For spinal cord slices, four slices (with thickness of 600 μm) were used in each condition. For each reaction in a 96-well plate, 100 μg of proteins, 100 μl of culture medium, or 5 μl of CSF (collected from cisterna magna 3 h after intrathecal injection of astrocytes) were used, and ELISA was performed according to the protocol of the manufacturer. The standard curve was included in each experiment.

Western blot

As we reported previously (Xu et al., 2013), spinal cord tissues (dorsal parts) or astrocyte cultures were homogenized in a RIPA lysis buffer (10×, Millipore) containing protease and phosphatase inhibitors.

Protein concentrations were determined by BCA Protein Assay (Pierce). Thirty micrograms of protein were loaded for each lane and separated by SDS-PAGE gel (4–15%; Bio-Rad). After the transfer, the blots were incubated overnight at 4°C with polyclonal antibody against Cx43 (1:2000, rabbit; Sigma), CXCL1 (1: 1000, rabbit; Boster). For loading control, the blots were probed with GAPDH antibody (1:20 000, mouse; Millipore). These blots were further incubated with horseradish peroxidase-conjugated secondary antibody (1:2000, GE Healthcare) developed in ECL solution (Thermo), and exposed onto ChemiDoc^{TM} MP Imaging System (Bio-Rad) for 1–10 min. Specific bands were evaluated by apparent molecular size. The intensity of the selected bands was analysed using NIH ImageJ software (http://rsb.info.nih.gov/ij/index.html). The same size boxes were used to select positive bands.

Immunohistochemistry and immunocytochemistry

As we reported previously (Gao et al., 2009) animals were deeply anaesthetized with isoflurane and perfused through the ascending aorta with PBS, followed by 4% paraformaldehyde with 1.5% picric acid in 0.16 M phosphate buffer. After the perfusion, the L4–L5 spinal cord segments were removed and post-fixed in the same fixative overnight. Spinal cord sections (30 μm, free-floating) were cut in a cryostat and processed for immunohistochemistry as we described previously (Xu et al., 2013). The sections were first blocked with 2% goat serum for 1 h at room temperature. The sections were then incubated overnight at 4°C with the following primary antibodies: GFAP antibody (1:1000, mouse; Millipore Bioscience Research Reagents), Cx43 antibody (1:1000, rabbit; Sigma), NeuN antibody (1:1000, mouse; Millipore Bioscience Research Reagents), CXCL1 (1: 200, rabbit; Boster), and CXCR2 antibody (1: 200, rabbit; Boster). The sections were then incubated for 1 h at room temperature with cyanine 3 (Cy3)- or FITC-conjugated secondary antibodies (1:400; Jackson ImmunoResearch). For double immunofluorescence, sections were incubated with a mixture of polyclonal and monoclonal primary antibodies, followed by a mixture of FITC- and Cy3-conjugated secondary antibodies. The stained sections were examined with a Nikon fluorescence microscope, and images were captured with a CCD Spot camera. We collected eight spinal cord sections from each mouse for quantification of immunofluorescence. Some sections were also evaluated with a confocal microscope (Zeiss 510 inverted confocal). The specificity of the antibodies was tested in our previous studies (Chen et al., 2012; Zhang et al., 2013).

For immunocytochemistry, cultured astrocytes, after incubation with TNF-α, were fixed with 4% paraformaldehyde for 20 min and processed for immunofluorescence with Cx43 (1:1000, rabbit; Sigma) and GFAP (1:1000, mouse; Millipore) antibody as shown above. To detect the contamination of fibroblasts in astrocyte cultures, we also performed double staining with GFAP antibody (1:1000, rabbit; Millipore) and FGFR4 antibody (1:100, mouse, Abcam). After immunostaining, 4′, 6′-diamidino-2-phenylindole (DAPI; 0.1 μg/ml; Sigma) was added for 5 min at room temperature to stain all the nuclei of cells in the cultures.

Gap junction function analysis in astrocytes

To determine the gap junction function in astrocytes, Lucifer yellow (5% in 1 M lithium chloride, Sigma) was microinjected to cultured astrocytes via a glass pipette (diameter of 2–4 μm) used for

patch-clamp recordings (Park *et al*., 2011). Diffusion of the dye to the neighbouring astrocytes was observed for 10 min. Some astrocytes were stimulated with TNF-α (10 ng/ml, 60 min) before the dye delivery. The images of labelled astrocytes were captured with a CCD Spot camera and the number of labelled astrocytes was quantified with the NIH ImageJ software.

Hemichannel function analysis in astrocytes

As hemichannels are permeable to the dye ethidium bromide, we used ethidium bromide uptake to measure the function of hemichannels. Astrocytes were stimulated with TNF-α for 1 h and exposed to 0.5 μM ethidium bromide (Sigma) for 10 min at 37°C. Then, cells were washed with Hank's balanced salt solution (HBSS) and supplemented with 1.2 mM CaCl$_2$ (HBSS-Ca^{2+}, Gibco). Astrocytes were examined with a Nikon fluorescence microscope, and images were captured with a CCD Spot camera. The positive staining of ethidium bromide was analysed with NIH ImageJ software.

Spinal cord slice preparation

As we reported previously (Park *et al*., 2011), a portion of the lumbar spinal cord (L4–L5) was removed from mice under urethane anaesthesia (1.5–2.0 g/kg, intraperitoneally) and kept in pre-oxygenated ice-cold Krebs' solution. Spinal segment was placed in a shallow groove formed in an agar block and glued to the bottom of the microslicer stage. Transverse slices (600 μm) were cut on a vibrating microslicer. The slices were perfused with Krebs' solution (8 ml/min) saturated with 95% O$_2$ and 5% CO$_2$ at 36 $\pm$ 1°C for at least 1–3 h before experiment. The Krebs' solution contained the following (in mM): 117 NaCl, 3.6 KCl, 2.5 CaCl$_2$, 1.2 MgCl$_2$, 1.2 NaH$_2$PO4, 25 NaHCO$_3$, and 11 glucose.

Patch-clamp recordings in spinal cord slices

The whole-cell patch-clamp recordings were made from lamina IIo neurons in voltage-clamp mode (Kawasaki *et al*., 2008; Park *et al*., 2011). Under a dissecting microscope with transmitted illumination, the substantia gelatinosa (lamina II) is clearly visible as a relatively translucent band across the dorsal horn. Patch pipettes were fabricated from thin-walled, borosilicate, glass-capillary tubing (1.5-mm outer diameter; World Precision Instruments). After establishing the whole-cell configuration, neurons were held their holding potentials at −70 mV for recording spontaneous excitatory postsynaptic currents (EPSCs). The resistance of a typical patch pipette is 5–10 MΩ. The internal solution contained the following (in mM): 135 potassium gluconate, 5 KCl, 0.5 CaCl$_2$, 2 MgCl$_2$, 5 EGTA, 5 HEPES, and 5 ATP-Mg. Membrane currents were amplified with an Axopatch 200 A amplifier (Molecular Devices) in voltage-clamp mode. Signals were filtered at 2 kHz and digitized at 5 kHz. Data were stored with a personal computer using pClamp 6 software and analysed with Mini Analysis (Synaptosoft). Those cells that showed >5% changes from the baseline levels were regarded as responding ones (Kawasaki *et al*., 2008).

Behavioural analysis

Animals were habituated to the testing environment daily for at least 2 days before baseline testing. The room temperature and humidity remained stable for all experiments. For testing mechanical sensitivity, animals were put in boxes on an elevated metal mesh floor and allowed 30 min for habituation before examination. The plantar surface of each hindpaw was stimulated with a series of von Frey hairs with logarithmically incrementing stiffness (0.02–2.56 g; Stoelting), presented perpendicular to the plantar surface (3–5 s for each hair). Based on Dixon's up-down method (Dixon, 1980), six von Frey tests were performed in each animal and the 50% paw-withdrawal threshold was determined. The observer was blinded to the treatment.

Quantification and statistics

All data were expressed as mean $\pm$ SEM. Six to nine separate astrocyte cultures from different animals were included for data analyses. Differences between groups were compared using Student's *t*-test or ANOVA, followed by Newman–Keuls test. The criterion for statistical significance was $P < 0.05$.

Results

Nerve injury induces a persistent upregulation of connexin-43 in spinal cord dorsal horn astrocytes

After CCI, neuropathic pain was shown to fully develop at 10 days and persist at 21 days (Xu *et al*., 2013). In the present study, we therefore used western blot analysis to examine Cx43 expression in the spinal cord dorsal horn at 10 and 21 days after CCI. Compared with sham surgery at the same time points, CCI induced marked increases in Cx43 expression at both the time points examined. This increase was significant at 10 days (1.77 $\pm$ 0.06-fold of sham, $P < 0.05$, $n = 4$ mice) and remained at peak levels at 21 days (1.74 $\pm$ 0.05-fold of sham, $P < 0.05$, $n = 4$ mice) (Fig. 1A and B). Immunohistochemistry in spinal cord sections of CCI mice showed that Cx43 in the dorsal horn was co-localized with GFAP (Fig. 1C), but not with the neuronal marker NeuN (Fig. 1D) and microglial marker CX3CR1 (using *Cx3cr1*-GFP mice) (Fig. 1E). Quantification of immunohistochemistry in the dorsal horn confirmed the upregulation of Cx43 and GFAP on the ipsilateral side 10 and 21 days after CCI when compared with the contralateral side (Supplementary Fig. 1, Fig. 1F and G) or sham surgery control (2.05 $\pm$ 0.19-fold increase for Cx43 and 2.27 $\pm$ 0.18-fold increase for GFAP in the late-phase, $P < 0.05$, $n = 4$). These findings suggest that CCI induces a long-lasting increase of Cx43 in spinal cord dorsal horn astrocytes, which is associated with long-lasting neuropathic pain in this model (Xu *et al*., 2013).

Spinal injection of carbenoxolone and connexin-43 mimetic peptides reduces chronic constriction injury-induced mechanical allodynia in late-phase neuropathic pain

We next tested whether Cx43 blockade could reverse late-phase neuropathic pain using several pharmacological approaches. First, we treated mice exhibiting symptoms of neuropathic pain with CBX (0.5 μg = 0.8 nmol, or 5 μg = 8 nmol, in 10 μl), a non-selective gap-junction inhibitor, 21 days after CCI. As shown in Fig. 2A,
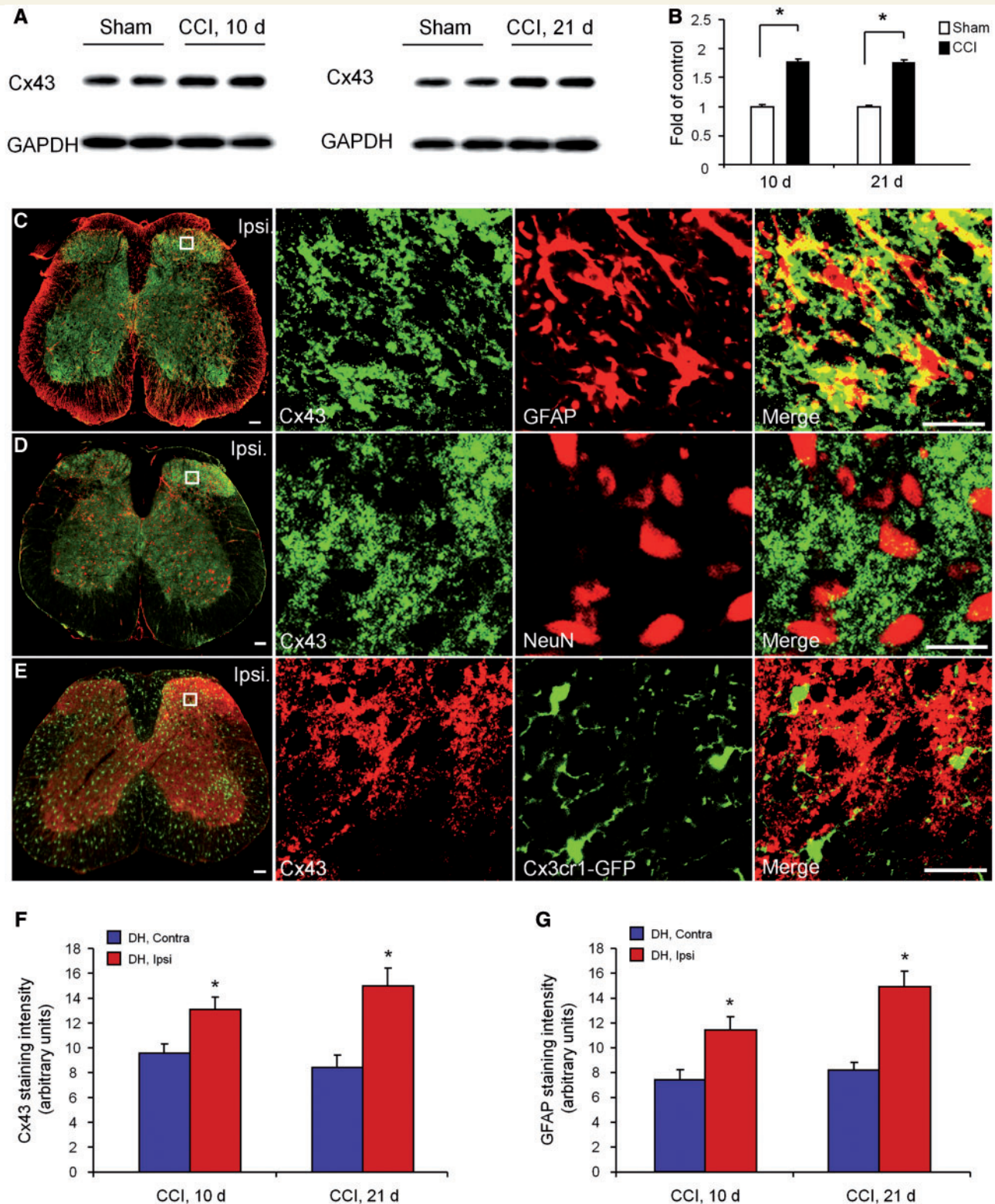
Figure 1 Nerve injury induces persistent upregulation of Cx43 in astrocytes of the spinal cord dorsal horn. (**A**) Cx43 expression in the spinal cord dorsal horn, as shown by western blotting, at 10 and 21 days after CCI and sham surgery. (**B**) Quantification of Cx43 levels in the dorsal horn. The western blot results are presented as a fold of sham control. *$P < 0.05$, compared with sham group, Student's t-test, $n = 4$ mice/group. (**C–E**) Confocal images in the dorsal horn 21 days after CCI show co-localization of Cx43 with GFAP (red, **C**) but not with the neuronal marker NeuN (red, **D**) and microglial marker CX3CR1 (green, **E**). Scale bar = 100 μm. (**F** and **G**) Quantification of Cx43 (**F**) and GFAP (**G**) immunoflurorescence intensity in the ipsilateral (Ipsi) and contralateral (Contra) superficial dorsal horn (DH) 10 and 21 days after CCI. *$P < 0.05$, compared with the contralateral group, Student's t-test, $n = 4$ mice/group. All data are mean ± SEM.
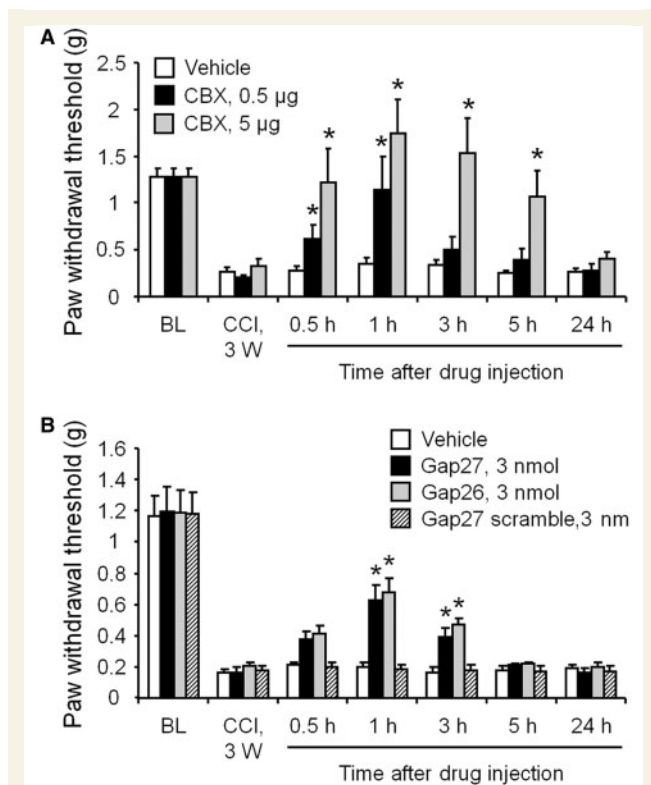
Figure 2 Spinal injection of CBX and Cx43 mimetic peptides 21 days after nerve injury reduces CCI-induced mechanical allodynia in the late phase. (**A**) Intrathecal injection of CBX (0.5 or 5 µg) rapidly (<0.5 h) and completely reversed mechanical allodynia for 5 h, in a dose-dependent manner. This inhibitory effect recovered after 24 h. (**B**) Intrathecal injection of Cx43 mimetic peptides ([43]Gap26, or [37,43]Gap27) also reduced mechanical allodynia for 3 h. However, the scrambled peptide (Gap27 scrambled) had no effect. All data are mean ± SEM. The differences between groups were analysed by ANOVA. *$P < 0.05$, compared with vehicle, $n = 6$–7 mice/group.

intrathecal CBX rapidly (<5 h) reversed mechanical allodynia for >5 h, in a dose-dependent manner. This reversal recovered after 24 h (Fig. 2A). As CBX is not selective for Cx43 and may affect other hemichannels such as pannexins (Chekeni *et al.*, 2010), we further tested the effects of Cx43 mimetic peptides ([43]Gap26 or [37,43]Gap27) and scrambled control peptide (Gap27 scrambled) (Retamal *et al.*, 2007; Wang *et al.*, 2012). Intrathecal injection of Cx43 mimetic peptides, but not the scrambled peptide, also reduced mechanical allodynia for 3 h (Fig. 2B). Because CBX is more effective in suppressing allodynia than Cx43 mimetic peptides, it may hit targets other than Cx43. Together these data suggest that Cx43 is required for the late-phase maintenance of neuropathic pain.

Spinal cord astrocytes and microglia are differentially involved in late-phase neuropathic pain

To further investigate the distinct roles of spinal astrocytes and microglia in late-phase neuropathic pain, we tested the effects of

the astroglial toxin L-α-aminoadipate (50 nmol) (Zhuang *et al.*, 2006) and microglial inhibitor (minocycline) (100 nmol) (Wen *et al.*, 2011) on CCI-induced mechanical allodynia 21 days after nerve injury. The late-phase mechanical allodynia was reduced by L-α-aminoadipate, but not minocycline (Supplementary Fig. 2A). We have previously shown that induction of c-Jun N-terminal kinase (JNK) in spinal astrocytes after nerve injury contributes to neuropathic pain maintenance (Zhuang *et al.*, 2006). D-JNKI-1, a selective peptide inhibitor of JNK, at a low dose (4 nmol), reduced late-phase mechanical allodynia (Supplementary Fig. 2B). Nerve injury is also known to induce p38 MAPK in spinal microglia especially in the acute stages, although weak p38 activation in spinal cord microglia is still evident in the late-phase (21 days) (Ji and Suter, 2007). Intrathecal injection of the p38 inhibitor SB203580 (80 nmol) reduced CCI-induced mechanical allodynia in the early-maintenance phase (10 days), but not in the late-phase (21 days) (Supplementary Fig. 2C and D). Thus, astrocytic, but not microglial signalling in the spinal cord might play an important role in late-phase neuropathic pain.

Connexin-43 contributes to chronic constriction injury-induced synaptic plasticity in spinal cord nociceptive neurons in the late-phase

Spinal cord synaptic plasticity (central sensitization) plays an essential role in driving pain hypersensitivity (Ji *et al.*, 2003; Kuner, 2010). We have previously shown that spontaneous EPSCs in spinal cord lamina IIo neurons were increased in the early-phase of nerve injury (3 days) (Xu *et al.*, 2013). In the present paper we therefore further investigated whether CCI would produce a long-lasting increase in spontaneous EPSCs. Spinal cord slices from sham and CCI mice (21 days) were prepared for patch-clamp recordings in lamina IIo neurons which receive C-fibre nociceptive input and also make synapses with lamina I projection neurons (Todd, 2010; Park *et al.*, 2011). Compared with sham surgery, CCI induced a profound increases in spontaneous EPSC frequency (from 6.6 ± 0.4 Hz to 14.9 ± 0.6 Hz, $P < 0.05$, $n = 5$ neurons) (Fig. 3A and B), indicating that nerve injury is associated with long-lasting increases in spinal cord synaptic transmission. Of interest, superfusion of spinal cord slices with CBX (10 µM) significantly inhibited the CCI-induced spontaneous EPSC frequency increase (Fig. 3A and B). Similarly, Cx43 mimetic peptide (Gap27, 100 µM) also reduced spontaneous EPSC frequency after CCI, without changing spontaneous EPSC frequency in sham controls (Fig. 3A and B). For comparison, superfusion of the scrambled peptide (Gap27 scrambled, 100 µM) had no effects on spontaneous EPSC frequency in both CCI and sham conditions (Fig. 3A and B). CCI also increased the amplitude of spontaneous EPSCs on Day 21, which was not affected by CBX and Cx43 mimetic peptide, suggesting a unique role of Cx43 in regulating spontaneous EPSC frequency (Fig. 3A and C).
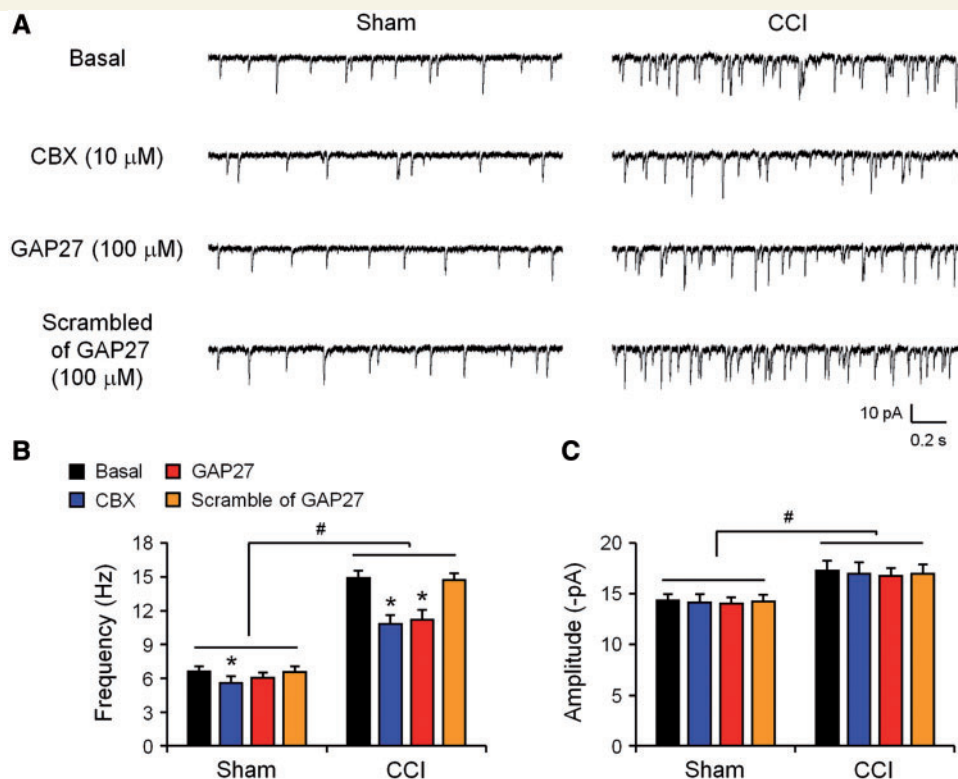
Figure 3 Cx43 inhibition 21 days after nerve injury reverses CCI-induced increase in spontaneous EPSCs in lamina II neurons of spinal cord slices. (**A**) Traces of spontaneous EPSCs. (**B**) Frequency of spontaneous EPSCs. CCI induced profound increases in spontaneous EPSC frequency in the late-phase, which is suppressed by CBX (10 μM) and Gap27 (100 μM). (**C**) spontaneous EPSC amplitude was not affected by CBX and Gap27. Note that superfusion of the scrambled peptide has no effects on the frequency and amplitudes of spontaneous EPSCs. *$P < 0.05$, compared with corresponding baseline (basal); [#]$P < 0.05$, compared with sham surgery, ANOVA followed by Newman–Keuls test, $n = 5$ neurons/group.

TNF-α induces CXCL1 release in astrocytes through connexin-43

To explore the molecular mechanisms by which astrocytic Cx43 regulates mechanical allodynia, we tested whether Cx43 was responsible for chemokine release in cultured astrocytes. As we previously reported (Gao *et al*., 2009; Zhang *et al*., 2013), brief incubation of astrocytes with TNF-α (10 ng/ml, 60 min at 37°C) substantially increased the release of CXCL1 (Fig. 4A and B). Notably, these increases were abolished by pretreatment of Cx43 blockers for 60 min. CBX (20 and 100 μM) dose-dependently suppressed the TNF-α-induced CXCL1 release in astrocytes (Fig. 4A). The Cx43 mimetic peptides, Gap26 (100 μM) and Gap27 (100 μM), also significantly inhibited the TNF-α-induced CXCL1 release, whereas Cx43 scrambled peptide (Gap27 scrambled, 100 μM) had no effects (Fig. 4B). Interestingly, probenecid (500 μM) and the PANX1 mimetic peptide [10]Panx1 (100 μM), two inhibitors of the pannexin hemichannels (Pelegrin and Surprenant, 2007; Chekeni *et al*., 2010) did not affect TNF-α-evoked CXCL1 release (Fig. 4A), arguing against the involvement of pannexins.

In addition to suppressing TNF-α-evoked CXCL1 release, CBX (100 μM) also inhibited the basal release of CXCL1 in astrocytes, in

the absence of TNF-α treatment (Fig. 4C). However, low concentration of CBX (20 μM) had no effects on basal release (Fig. 4C), although this dose inhibited TNF-α-evoked CXCL1 release (Fig. 4A).

Apart from triggering chemokine release, TNF-α also increased the cytosolic content of CXCL1 in astrocytes, indicating enhanced expression of CXCL1. TNF-α induced increases in CXCL1 was however not sensitive to CBX (Fig. 4D). Neither was the basal unstimulated content (basal expression) of CXCL1 reduced by CBX (Fig. 4E). In fact, CBX at a high dose (100 μM) increased CXCL1 content (Fig. 4D). Similarly, Cx43 inhibition reduced CCL2 release, but not content in TNF-α treated astrocytes (Supplementary Fig. 3A–E). Combined, these observations suggest that Cx43 controls the release of chemokines via a mechanism that is independent of protein synthesis.

To confirm a selective role of Cx43 in chemokine release, we also treated astrocyte cultures with a specific small interfering RNA that targets the carboxy-terminal region of Cx43 messenger RNA (Iacobas *et al*., 2008). Following the treatment of Cx43 small interfering RNA (1 μg/ml, 18 h), we found a 66% reduction in Cx43 expression in astrocyte cultures compared with non-targeting small interfering RNA treatment (Supplementary Fig. 4A). Notably, this small interfering RNA treatment also inhibited TNF-α-induced CCL2 and CXCL1 release by 53% and 47%,
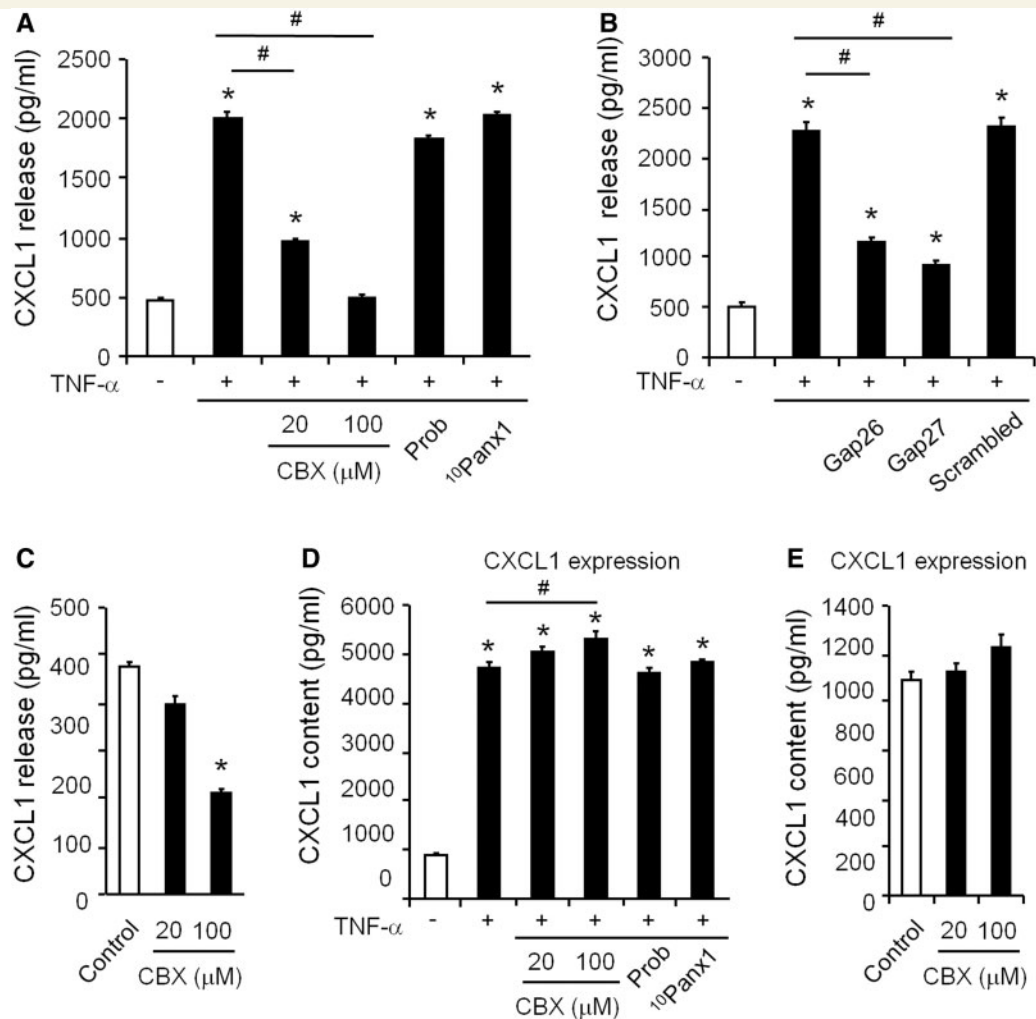
Figure 4 Cx43 is required for TNF-α-evoked and basal release of CXCL1 in astrocyte cultures. (**A** and **B**) CXCL1 release in astrocytes following TNF-α stimulation (10 ng/ml, 60 min). Note the TNF-α-induced CXCL1 release is suppressed by pretreatment (60 min) of CBX (20 and 100 μM, **A**) and Gap26 and Gap27 (100 μM, **B**) but not by the inhibitors of pannexin hemichannels probenecid (Prob, 500 μM, **A**) and PANX1 mimetic peptide [10]Panx1 (100 μM, **A**) and the scrambled peptide (Gap27 scrambled, 100 μM, **B**). *$P < 0.05$, compared with control; #$P < 0.05$, compared with TNF-α. (**C**) Inhibition of basal release of CXCL1 by CBX in astrocytes. *$P < 0.05$, compared with control. (**D**) Evoked expression (content) of CXCL1 in astrocytes following TNF-α stimulation (10 ng/ml, 60 min). Note the TNF-α-induced CXCL1 expression is not suppressed by pretreatment (60 min) of CBX (20 and 100 μM) and inhibitors of pannexin hemichannels probenecid (Prob, 500 μM) and PANX1 mimetic peptide [10]Panx1 (100 μM). In contrast, a high dose of CBX (100 μM) increases CXCL1 expression. *$P < 0.05$, compared with control; #$P < 0.05$, compared with TNF-α. (**E**) Effects of CBX on the basal expression (content) of CXCL1 in astrocytes. All data are mean ± SEM. $n = 8$ cultures/group. The differences between groups were analysed by ANOVA followed by Newman–Keuls test.

respectively. However, the non-targeting small interfering RNA did not alter CCL2 and CXCL1 release (Supplementary Fig. 4).

To validate that astrocytes from spinal cords have similar responses to TNF-α as astrocytes from the cortices, we prepared astrocyte cultures from spinal cords. Immunocytochemistry showed that >98% cells were positive for GFAP and only <2% cell were labelled with FGFR4, a marker for fibroblasts, confirming the identity of astrocytes (Supplementary Fig. 5A–F). ELISA analysis demonstrated that in cultured spinal cord astrocytes TNF-α also induced CXCL1 release, which was suppressed by Cx43 inhibitor Gap26 but not by pannexin inhibitor [10]Panx1

(Supplementary Fig. 5G). This result suggests that Cx43 is also critically required for TNF-α-induced CXCL1 release in spinal cord astrocytes.

We also used FACS to collect spinal cord astrocytes from adult *Gfap*-GFP mice. Successful sorting of astrocytes was validated by GFP staining (Supplementary Fig. 6A). Sorted cells were then incubated (30 000 cells in each group) with TNF-α for 30 and 60 min after pretreatment with Cx43 blockers. TNF-α also increased CXCL1 release in spinal cord astrocytes, and this increase was suppressed by CBX and the combined treatment of Gap26 and Gap27, but not by the scrambled peptide (Supplementary Fig. 6B).

Next we performed a similar experiment in spinal cord slices. TNF-α increased CCL2 and CXCL1 release in spinal cord slices, and again, these increases were reduced by CBX and the combined treatment of Gap26 and Gap27 (Supplementary Fig. 6C and D). Collectively, these data suggest that spinal cord astrocytes are able to release the chemokines CCL2 and CXCL1 through Cx43 following TNF-α stimulation.

TNF-α increases connexin-43 expression and hemichannel activity in astrocytes

Cx43 forms two types of channels in astrocytes: gap junction channels for direct intercellular communication between astrocytes and unopposed hemichannels that permit cytosolic exchanges with the extracellular space. Previous studies have documented an increase in astrocytic Cx43 expression after pathological events including spinal cord injury and peripheral nerve injury (Wu et al., 2011; Chen et al., 2012), however, the functional significance of this increase remains unclear. A prerequisite to answering this question is determining whether this increase corresponds to the recruitment of new gap junctions or unopposed hemichannels. We therefore investigated this question with the following set of experiments in astrocyte cultures.

To verify that treatment with a known inflammatory mediator, TNF-α, could directly reproduce pathological increases in Cx43 expression, we performed western blotting for Cx43. Our results show that TNF-α treatment (3 h) evoked a significant increase in Cx43 expression in astrocyte cultures (1.54 ± 0.03-fold of control, $P < 0.05$, $n = 6$ separate cultures) (Fig. 5A), and immunocytochemistry confirmed a similar increase (Fig. 5B). In contrast, the mix of cytokines IL1B and TNF-α treatment (24 h) was shown to reduce Cx43 expression in cultured astrocytes (Retamal et al., 2007). The discrepancy may result from different treatment and culture conditions of astrocytes (e.g. including dibutyrlyl-cAMP) in this study.

To detect the activity of gap junction channels, we microinjected Lucifer yellow, a gap junction-permeable dye, into an astrocyte, and the diffusion of the dye to adjacent astrocytes was examined. As shown in Fig. 5C and D, there was no difference between control and TNF-α (10 ng/ml, 60 min) treated group. Thus, TNF-α does not directly modulate gap junction communication in astrocytes. Notably, the mix of cytokines IL-1β and TNF-α treatment (24 h) was shown to reduce gap-junction activities (Retamal et al., 2007).

Ethidium bromide uptake was previously taken as an index for the activity of connexin hemichannels in astrocytes (Retamal et al., 2007). We therefore adopted this approach to differentiate between TNF-α-induced hemichannel activity and gap-junction communication. Under the control conditions and in the presence of external calcium, only small numbers of astrocytes exhibited ethidium bromide uptake (21.3 ± 2.6 positive cells/field; $n = 9$ cultures). However, 1 h after TNF-α treatment, there was a 2-fold increase in the number of ethidium bromide-positive cells (64.4 ± 8.3 positive cells/field; $n = 9$ cultures; $P < 0.05$) (Fig. 5E and F). Notably, Gap27 (100 μM), but not the scrambled peptide

(Gap27 scrambled, 100 μM), significantly inhibited the TNF-α-induced uptake of ethidium bromide (10.1 ± 1.6 ethidium bromide-positive cells/field after Gap27 treatment, $n = 9$ cultures; $P < 0.05$). Interestingly, Gap27 also suppressed the basal ethidium bromide uptake by 50% (Fig. 5E and F). These data suggest that TNF-α induces upregulations of astrocytic Cx43 expression that correspond to increased Cx43-mediated hemichannel activity but not gap-junction communication.

Spinal injection of TNF-α-activated astrocytes induces mechanical allodynia via connexin-43-mediated CXCL1 release

To determine if the astrocytic release mechanism we have revealed plays a role in chronic pain sensitization, we intrathecally injected activated astrocytes (known to be present in chronic pain) and measured astrocyte-induced mechanical allodynia. As we previously demonstrated (Gao et al., 2009), TNF-α-activated astrocytes elicited persistent mechanical allodynia for several days (Fig. 6A). To demonstrate a role of astrocytic Cx43 in generating mechanical allodynia, we first treated astrocyte cultures with Cx43 small interfering RNA or non-targeting control small interfering RNA (1 μg/ml) for 18 h. Astrocytes were then stimulated with TNF-α (10 ng/ml) for 15 min, washed with PBS three times to remove TNF-α in the medium, and collected for intrathecal injection in naïve mice. TNF-α-activated astrocytes were sufficient to induce mechanical allodynia for >48 h, and this allodynia was prevented by pretreatment of astrocytes with Cx43 small interfering RNA, but not non-targeting small interfering RNA treatment (Fig. 6A).

In light of these findings we reasoned that activated astrocytes might contribute to the maintenance of late-phase neuropathic pain through the release of CXCL1. Consistently, CXCL1 levels in CSF, collected from cisterna magna, were significantly increased 3 h after intrathecal injection of the activated astrocytes (Fig. 6B). Intrathecal injection of a CXCL1 neutralizing antibody (4 μg) transiently reversed mechanical allodynia induced by TNF-α-treated astrocytes (Fig. 6C). This reversal began at 1 h, maintained at 3 h and diminished at 24 h following the antibody injection (Fig. 6C). In contrast, intrathecal injection of the control IgG antibody had no effect on mechanical allodynia (Fig. 6C).

We next tested whether blocking CXCR2, a major receptor of CXCL1 (Horuk et al., 1997; Nguyen and Stangel 2001; Valles et al., 2006) would modulate astrocyte-induced pain hypersensitivity. Intrathecal injection of SB225002 (20 μg), a potent and selective CXCR2 antagonist (White et al., 1998; Zhang et al., 2013), reversed mechanical allodynia by TNF-α-activated astrocytes for >3 h (Fig. 6D). This result further supports the involvement of chemokine signalling in astrocytes-induced chronic pain.

CXCL1 signalling contributes to late-phase neuropathic pain

Western blotting showed a profound upregulation of CXCL1 in the spinal cord dorsal horn 21 days after CCI (Fig. 7A).
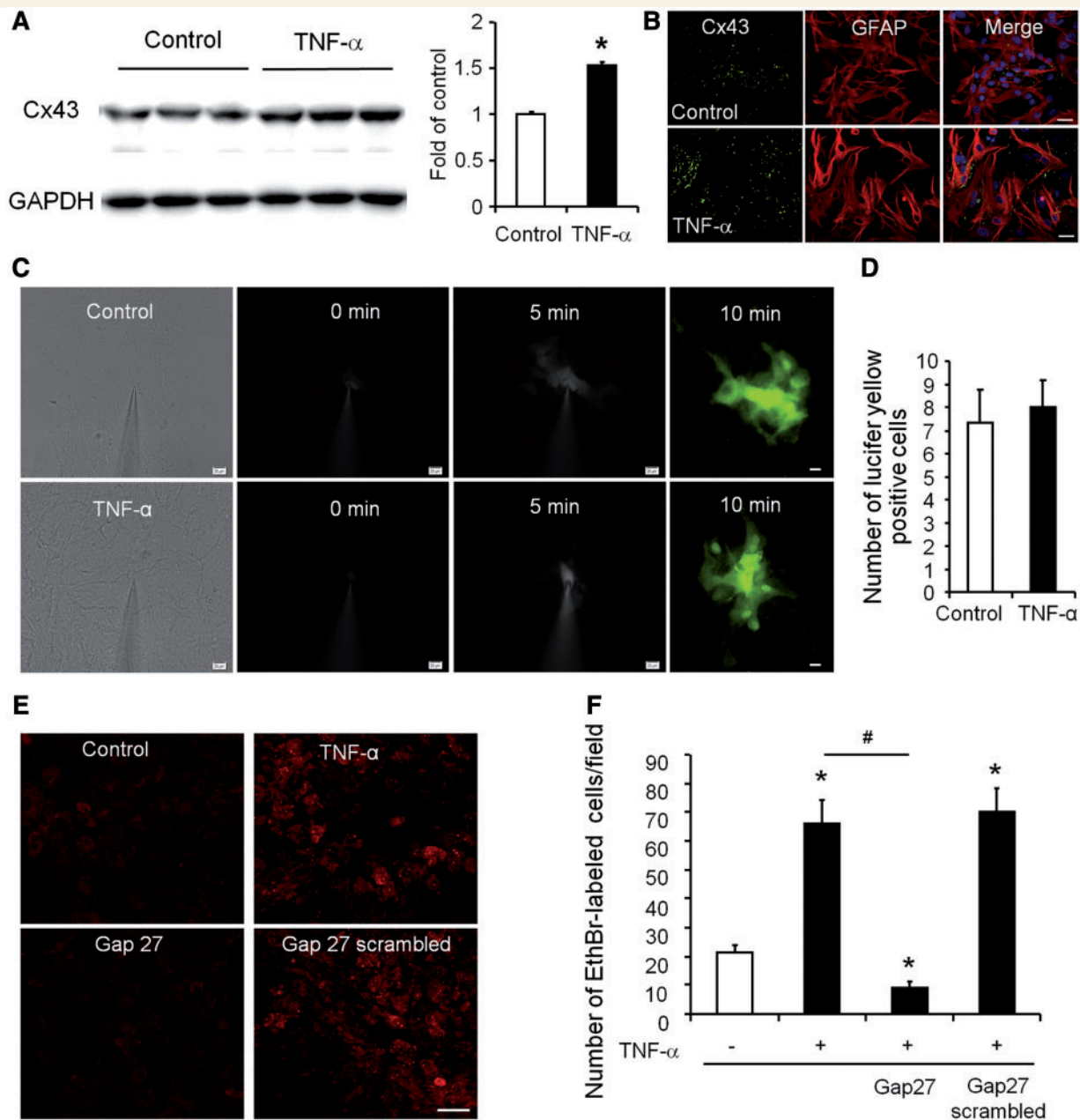
Figure 5 TNF-α increases Cx43 expression and hemichannel activity in cultured astrocytes. (**A**) TNF-α (10 ng/ml, 3 h) induces Cx43 expression (western blotting) in astrocyte cultures. *P < 0.05, compared with control, Student's *t*-test, n = 8 cultures/group. (**B**) Double staining showing increased Cx43 expression in GFAP-expressing astrocytes following the TNF-α treatment. Scale bar = 10 μm. (**C**) TNF-α treatment (10 ng/ml, 60 min) does not alter gap junction communication in astrocytes, revealed by diffusion of Lucifer yellow following microinjection into an astrocyte. Scale bars = 10 μm. (**D**) Number of Lucifer yellow-labelled astrocytes following dye injection into a single astrocyte. P > 0.05, compared with control, Student's *t*-test, n = 8 cultures/group. (**E**) TNF-α treatment (10 ng/ml, 60 min) increases hemichannel function revealed by ethidium bromide (EthrBr) uptake in astrocytes. Note this increases is suppressed by Gap27 (100 μM). Scale bar = 20 μm. (**F**) Number of ethidium bromide-positive astrocytes and the effects of TNF-α, Gap27 and its control peptide (scrambled Gap27, 100 μM). The differences between groups were analysed by ANOVA followed by Newman–Keuls test. n = 9 cultures/group. *P < 0.05, compared with control without treatment; #P < 0.05, compared with TNF-α group.

Intrathecal injection of CXCR2 antagonist SB225002 (20 μg) reduced mechanical allodynia in the late-phase for >3 h (Fig. 7B). Double immunostaining of CXCL1/GFAP and CXCR2/NeuN in the dorsal horn of CCI-21 days animals indicated that CXCL1 and CXCR2 were localized in spinal cord astrocytes and neurons, respectively (Fig. 7C and Supplementary Fig. 7A–C). Thus, CXCL1 induction in spinal astrocytes may sustain late-phase neuropathic pain by activating CXCR2 in neurons.
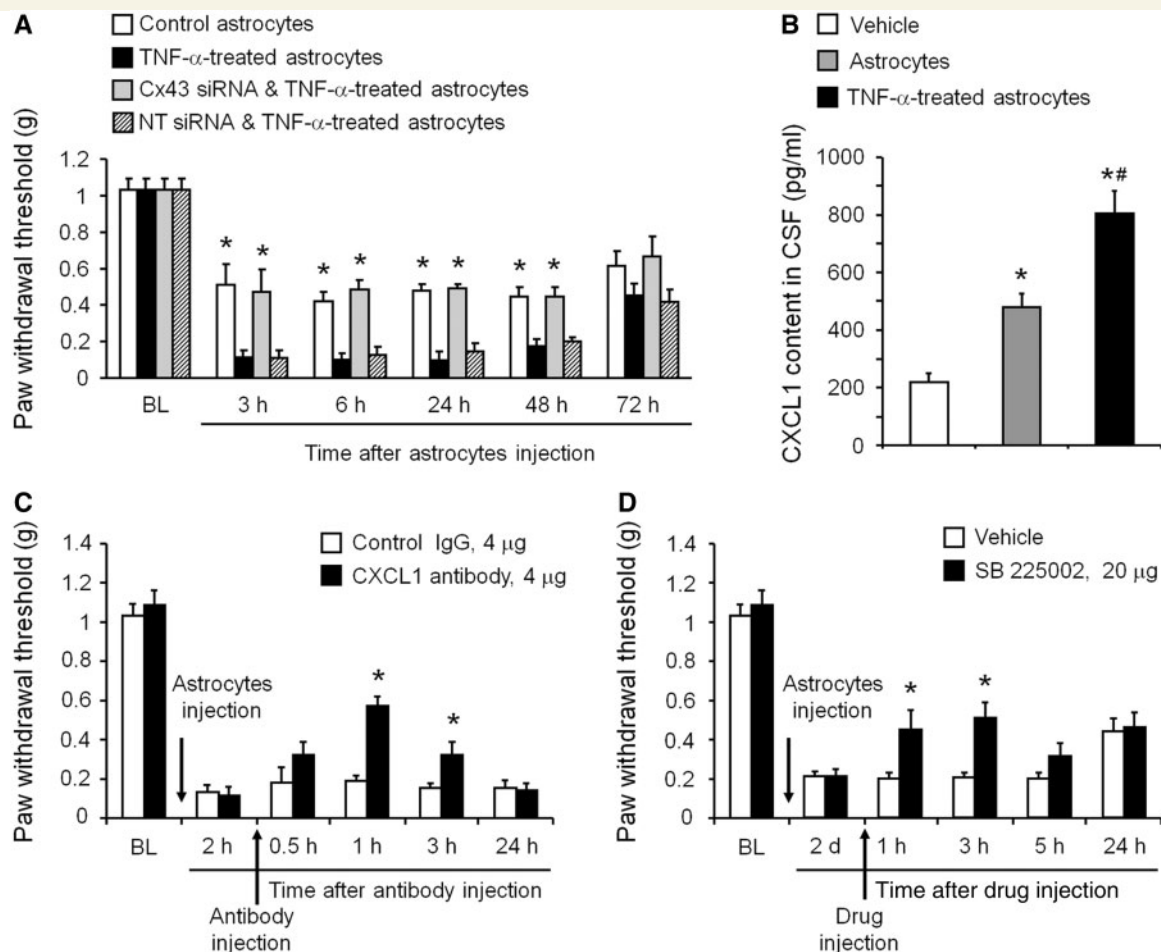
Figure 6 Spinal injection of TNF-α-activated astrocytes induces mechanical allodynia via Cx43-mediated CXCL1 release. (**A**) Intrathecal injection of TNF-α-activated astrocytes elicited persistent mechanical allodynia for >48 h. Note this allodynia is reduced by pretreatment of astrocytes with Cx43 small interfering RNA (1 μg/ml, 18 h). *$P < 0.05$, compared with TNF-α or TNF-α + non-targeting control small interfering RNA treated group; $n = 6$ mice/group. (**B**) ELISA analysis shows increased CXCL1 release in the CSF at 3 h after the intrathecal injection of TNF-α-activated astrocytes. *$P < 0.05$, compared with vehcile group; #$P < 0.05$, compared with non-activated astrocytes; $n = 4$ mice/group. (**C**) Intrathecal injection of a CXCL1 neutralizing antibody (4 μg) transiently and partially reversed mechanical allodynia, induced by TNF-α-treated astrocytes. *$P < 0.05$, compared with control IgG group; $n = 6$ mice/group. (**D**) Intrathecal injection of the CXCR2 antagonist SB225002 (20 μg = 57 nmol) transiently and partially reversed mechanical allodynia, induced by TNF-α-activated astrocytes. *$P < 0.05$, compared with vehicle (PBS); $n = 5$–6 mice/group. All data are mean ± SEM. The differences between groups were analysed by ANOVA followed by Newman–Keuls test.

CXCL1 enhances excitatory synaptic transmission in spinal cord neurons via CXCR2

To dissect the synaptic mechanisms underlying CXCL1-elicited pain, we investigated the impact of CXCL1 on spontaneous EPSCs in lamina IIo neurons of spinal cord slices. CXCL1 superfusion (100 ng/ml) immediately increased spontaneous EPSC frequency (Fig. 7D and E). Interestingly, CCI-induced spontaneous EPSC frequency increase in the late phase (21 days) was suppressed by the CXCR2 antagonist SB225002 (1 μM, Fig. 7F and G), indicating a possible role of endogenous CXCL1 in regulating nerve injury-induced synaptic plasticity in the late-phase. Collectively, these findings indicated that CXCL1 can directly

modulate synaptic transmission to sustain late-phase neuropathic pain via activation of neuronal CXCR2.

Discussion

In this study, we have demonstrated a novel mechanism of astrocytic Cx43 hemichannels in maintaining nerve injury-induced late-phase neuropathic pain. The same mechanism produced spinal cord synaptic plasticity via chemokine-mediated neuron-glial interactions. The mechanism was dissected through multiple experimental approaches: First, CCI elicited a persistent (>21 days) upregulation of Cx43 in spinal cord astrocytes. Second, spinal injection of CBX and the Cx43 blocking/mimetic peptides Gap26 and Gap27 effectively reduced the neuropathic pain symptom
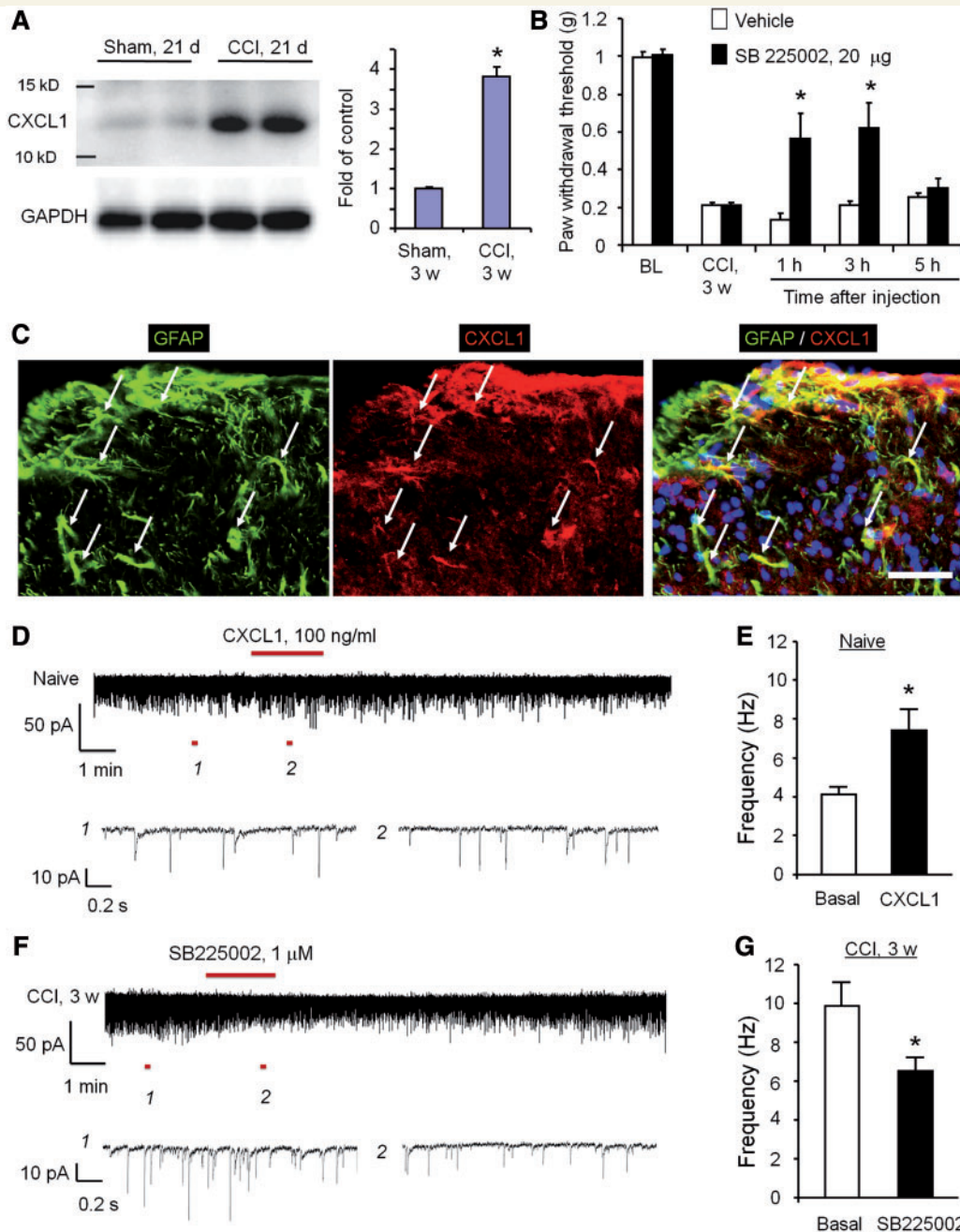
Figure 7 CXCL1, upregulated in spinal cord astrocytes after nerve injury, enhances excitatory synaptic transmission in spinal cord neurons and maintains neuropathic pain via CXCR2. (**A**) Western blotting shows CXCL1 upregulation in the spinal cord dorsal horn 21 days after CCI. *Right*, quantification of Cx43 levels in the dorsal horn. The western blot results are presented as a fold of sham control. *$P < 0.05$, compared to sham control, Student's *t*-test, $n = 4$ mice/group. (**B**) Intrathecal injection of SB 225002 (20 µg), 21 days after CCI, reduced CCI-induced mechanical allodynia in the late phase. *$P < 0.05$, compared with vehicle (saline), Student's *t*-test, $n = 6$ mice/group. (**C**) Double immunostaining of CXCL1 and GFAP in the dorsal horn 21 days after CCI. Note CXCL1 is primarily colocalized with GFAP. Arrows indicate doubled-labelled cells. Scale bar = 50 µm. (**D** and **E**) CXCL1 superfusion (100 ng/ml) increases spontaneous EPSC frequency (revealed by patch clamp recordings) in lamina IIo neurons of spinal cord slices. (**E**) Spontaneous EPSC frequency. *$P < 0.05$, Student's *t*-test, $n = 5$ neurons/group. (**F** and **G**) CCI (21 d) increases spontaneous EPSC frequency, which is reversed by the CXCR2 antagonist SB225002 (1 µM). *$P < 0.05$, Student's *t*-test, $n = 5$ neurons/group.

(mechanical allodynia) in the late phase (21 days). Third, nerve injury induced a profound and persistent increase in spontaneous EPSCs in lamina IIo neurons of spinal cord slices, and this increase was suppressed by CBX and Gap26/Gap27. Fourth, TNF-α

increased Cx43 hemichannel, but not gap-junction activities in cultured astrocytes and induced substantial release of the chemokines CCL2 and CXCL1 in astrocytes via Cx43. Fifth, spinal injection of TNF-α-activated astrocytes was sufficient to induce

persistent mechanical allodynia, which was reduced by Cx43-small interfering RNA pretreatment and reversed by the CXCL1 neutralizing antibody and the CXCL1 receptor (CXCR2) antagonist. Finally, CXCL1 increased spontaneous EPSC frequency in lamina IIo neurons, and conversely the CXCR2 antagonist suppressed CCI-induced spontaneous EPSC frequency increase and neuropathic pain in the late-phase.

Spinal cord astrocytes, connexin-43 and late-phase neuropathic pain

The emerging literature strongly implicates a role for spinal cord glia, especially microglia and astrocytes in the genesis and maintenance of neuropathic pain (Tsuda et al., 2005; Watkins and Maier, 2005; Gao and Ji, 2010b; Ren and Dubner, 2010; Chiang et al., 2012; Ji et al., 2013). Microglia and astrocytes play distinct roles in neuropathic pain induction and maintenance (Raghavendra et al., 2003; Shi et al., 2012). Compared to microglial activation, astroglial activation in neuropathic pain conditions is more persistent and plays a more important role in neuropathic pain maintenance (Raghavendra et al., 2003; Zhang and De Koninck, 2006; Shi et al., 2012; Ji et al., 2013), although microglia are also involved in neuropathic pain maintenance (Tsuda et al., 2003; Katsura et al., 2006; Clark et al., 2007; Ji and Suter, 2007; Kobayashi et al., 2008).

Notably, behavioural tests for neuropathic pain maintenance were primarily performed in the first 2 weeks of nerve injury in previous studies (Jin et al., 2003; Tsuda et al., 2003, 2011; Clark et al., 2007; Kawasaki et al., 2008). To determine the unique role of microglia and astrocytes in the late-phase neuropathic pain, we examined CCI-induced mechanical allodynia, a cardinal feature of chronic neuropathic pain, 3 weeks after nerve injury. As expected, astroglial toxin L-α-aminoadipate but not microglial inhibitor minocycline reduced this late-phase neuropathic pain (Supplementary Fig. 2A). Consistently, previous studies showed that delayed minocycline treatment only inhibited heat hyperalgesia but not mechanical allodynia (Mei et al., 2011; Vanelderen et al., 2013). Although intrathecal p38 inhibitor SB203580 reduced mechanical allodynia on Day 10 (Jin et al., 2003), it did not affect allodynia on Day 21 (Supplementary Fig. 2C and D). In contrast, spinal inhibition of JNK, induced in astrocytes after nerve injury (Zhuang et al., 2006), was still effective in reducing the late-phase neuropathic pain (Supplementary Fig. 2B). These findings indicate that astrocytes and astrocytic signalling could be critical for driving late-phase neuropathic pain. In particular, we demonstrated that Cx43 is also critically involved in late-phase neuropathic pain.

Cx43 and Cx30 are the principal connexins expressed by astrocytes and Cx43 is upregulated in the spinal cord after peripheral nerve injury (Wu et al., 2011; Yoon et al., 2013) and spinal cord injury (Chen et al., 2012). Inhibition of Cx43 was shown to protect ischaemia (Rami et al., 2001), attenuate inflammation, improve functional recovery following spinal cord injury (Chen et al., 2012; Huang et al., 2012), and block the development of central neuropathic pain after spinal cord injury (Chen et al., 2012). These reports are consistent with accumulating evidence from multiple groups suggesting the Cx43 contributes to the

development of neuropathic pain (Spataro et al., 2004; Ohara et al., 2008; Yoon et al., 2013). Notably, spinal cord injury-induced central neuropathic pain was abolished in Cx43/Cx30 double knockout mice but not in Cx30 knockout mice (Chen et al., 2012). The present study showed that persistent upregulation of Cx43 in spinal cord astrocytes (>3 weeks) is required for generating late-phase neuropathic pain (Fig 2). In addition to CBX, an extensively used but non-selective blocker of Cx43 (Spataro et al., 2004), we also tested the mimetic peptides [43]Gap26 and [37,43]Gap27 for more selective blockade of Cx43 (Retamal et al., 2007). Both CBX and the mimetic peptides reversed CCI-induced neuropathic pain in the late-phase (Fig. 2). However, we should not rule out that CBX may inhibit pain by hitting other targets.

Connexin-43 hemichannels and chemokine release in astrocytes

Apart from forming gap junctions, Cx43 also forms unopposed hemichannels, providing a pathway for molecular exchange between the cytoplasm and the extracellular compartment (Saez et al., 2005). Under the resting conditions, these hemichannels, located at non-opposed plasma membrane domains, present a low open probability that can be modulated in the inflammatory and stress conditions (Contreras et al., 2002; Saez et al., 2005; Retamal et al., 2007). We found that TNF-α increased Cx43 expression and Cx43-mediated hemichannel activity in astrocytes (Fig. 5). The opening of the hemichannels allows the release of small molecules such as ATP and glutamate (Stout et al., 2002; Ye et al., 2003; Bennett et al., 2012) providing a paracrine route for intercellular communication. Interestingly, several studies have shown a switch between two functional properties of Cx43 channels in well-defined conditions. For instance, the proinflammatory cytokines IL-1β and TNF-α reduced the Cx43-mediated gap junction communication (GJC), but increased the Cx43-mediated hemichannel activity (Retamal et al., 2007). Injury-induced upregulation of Cx43 is associated with a diminishing of normal gap junction communication (Contreras et al., 2002; Garré et al., 2010). Our data showed that a brief (1 h) treatment of TNF-α did not change gap junction communication but increased Cx43-mediated hemichannel activity (Fig. 6C–F). These observations are consistent with the hypothesis that it is upregulation of Cx43 hemichannels and enhanced release of astrocytic signalling molecules that is causally implicated in chronic pain, rather than a downregulation of gap junction coupling or a change in gap junction communication.

One of the most striking findings in this study is the critical involvement of Cx43 but not pannexin hemichannels in TNF-α-induced release of the chemokines (CCL2 and CXCL1) in cultured astrocytes, FACS-selected spinal cord astrocytes, and spinal cord slices. TNF-α-induced chemokine release was blocked by Cx43 small interfering RNA, CBX and Gap26/Gap27, indicating a selective role of Cx43. Cx43 was also required for the basal release of CCL2 and CXCL1 in astrocytes. Interestingly, Cx43 was not required for inducing the expression of CCL2 and CXCL1 in astrocytes following stimulation of TNF-α. Hence Cx43 is involved in the release but not the increase in the cytosolic content of CCL2

and CXCL1 in response to TNF-α exposure. Importantly, Cx43-mediated astrocytic CXCL1 release is sufficient to induce mechanical allodynia, as the CXCL1 neutralization could partially reverse activated astrocytes-induced allodynia. Although hemichannels are generally thought to facilitate direct transfer of small molecules and ions <1 kDa, Cx43 is also known to control the secretion of CXCL12 in bone marrow stromal cells (Schajnovitz *et al.*, 2011). Furthermore, CBX was shown to reduce IL-1β and IL6 release in the CSF, in response to intrathecal HIV1 gp120 (Spataro *et al.* 2004). Although chemokines are small molecular weight polypeptides, their size is too large to allow direct efflux via Cx43 hemichannels. It is likely that nerve injury-induced hyperactivity of Cx43-mediated hemichannels makes astrocytes 'leaky' through cytoskeleton changes (Cotrina *et al.*, 2000). Future studies are needed to establish how Cx43 hemichannels regulates the release of small polypeptides. Given the role of purinergic signalling in astrocytic release, it is tempting to speculate that the increase in purine mediated signalling associated with Cx43 expression may regulate the release of chemokines.

Cx43- and chemokine-mediated astrocytic-neuronal interactions in late-phase neuropathic pain

Spinal cord synaptic plasticity (central sensitization) plays an essential role in driving neuropathic pain (Ji *et al.*, 2003; Costigan *et al.*, 2009; Kuner, 2010). In this study we focused on lamina IIo interneurons for the following reasons. First, these are predominantly excitatory neurons expressing vesicular glutamate transporter 2 (now known as SLC17A6; Park *et al.*, 2011). Second, they form a nociceptive circuit by receiving input from TRPV1-positive C-fibres and synapse with lamina I projection neurons (Todd, 2010; Park *et al.*, 2011). Third, they demonstrated robust changes (increased EPSCs) in inflammatory and neuropathic pain conditions (Xu *et al.*, 2013; Berta *et al.*, 2014). In particular, our data show that CCI produced a persistent increase in spontaneous EPSC frequency (>3 weeks) in spinal cord lamina IIo neurons (Fig. 3). Cx43 could directly modulate this long-term synaptic plasticity, since the spontaneous EPSC frequency increase was suppressed by CBX and Gap27 (Fig. 3). These findings provide a synaptic mechanism by which Cx43 controls late-phase neuropathic pain. CBX treatment also significantly attenuated the nerve injury-induced mechanical hypersensitivity and central sensitization parameters (increased receptive field size, reduction of mechanical activation threshold and increases in noxious stimulation-evoked responses) in the trigeminal system (Wang *et al.*, 2014). Cx43-mediated enhancement of excitatory synaptic transmission can be recapitulated by CXCL1, as superfusion of spinal cord slices with CXCL1 induced a significant and rapid (within 1 min) increase in spontaneous EPSC frequency (Fig. 7). Conversely, CCI-induced increases in spontaneous EPSC frequency in the late-phase was reversed by blocking the major receptor of CXCL1 (CXCR2) with SB225002 (Fig. 7).

Recent studies have indicated an important role of chemokines in neuropathic pain (White *et al.*, 2007; Zhang *et al.*, 2007; Gao and Ji, 2010*a*). Nerve injury induces upregulations of CCL2 (Gao *et al.*, 2009), CCL7 (Imai *et al.*, 2013) and CXCL1 (Zhang *et al.*, 2013; Manjavachi *et al.*, 2014) in spinal cord astrocytes to maintain neuropathic pain. Spinal CXCL1 upregulation persists 3 weeks after nerve injury and double-staining showed that CXCL1 is primarily expressed in spinal astrocytes. Notably, intrathecal injection of the CXCR2 antagonist SB225002 reduced neuropathic pain in the late-phase. Consistently, mechanical allodynia, induced by the activated astrocytes, was also inhibited by SB225002, the CXCL1 antibody, and the Cx43 small interfering RNA. Together, these results suggested that the activated astrocytes could promote late-phase neuropathic pain via Cx43-mediated CXCL1 release to enhance excitatory synaptic transmission in the pain circuitry of the superficial dorsal horn. Given a well-documented role of astrocytic Cx43 in controlling the release of ATP (Cotrina *et al.*, 2000; Kang *et al.*, 2008) and a critical role of ATP in the activation of spinal cord microglia via P2RX4 (Tsuda *et al.*, 2003), P2RX7 (Kobayashi *et al.*, 2011), and P2RY12 (Kobayashi *et al.*, 2008; Tozaki-Saitoh *et al.*, 2008) and the development of neuropathic pain, astrocytic Cx43 should also modulate microglial activation via ATP release.

Conclusions and clinical relevance

We have demonstrated a unique role of Cx43-mediated hemichannels in spinal cord astrocytes for driving late-phase neuropathic pain after peripheral nerve injury. Mechanistically, Cx43 controls the astrocytic release of CXCL1, and CXCL1 maintains late-phase spinal cord synaptic plasticity by activating CXCR2 receptors in primary afferent neuron central terminals and dorsal horn neurons in the spinal cord (Fig. 8). Future studies are warranted to fully investigate how Cx43-mediated hemichannels control chemokine release. Given the important roles of glial cells in the pathogenesis in neuropathic pain, glia-targeting drugs may help alleviate neuropathic pain. However, lessons should be learned from the recent clinical trials with glia-targeting drugs in patients with neuropathic pain (Ji *et al.*, 2013). These drugs include the glial modulator propentofylline (Landry *et al.*, 2012), the CCR2 antagonist AZD2423 (Kalliomaki *et al.*, 2013), and the p38 inhibitor losmapimod (Ostenfeld *et al.*, 2013), which only show limited effects, although the p38 inhibitor dilmapimod (SB-681323) produces significant reduction in nerve injury-induced neuropathic pain (Anand *et al.*, 2011). The lack of efficacy of these glial targeting drugs could reflect inadequate exposure at central sites (Gao and Ji, 2010*a*; Ji *et al.*, 2013; Ostenfeld *et al.*, 2013) or that neuropathic pain mechanisms in the late phase differ fundamentally from those established at earlier time points. Our data suggest that targeting neuropathic pain mechanisms in the late-phase through astrocytic release with CNS permeable drugs may lead to more effective therapies for the management of chronic neuropathic pain. In particular, upregulation of Cx43 hemichannels is a stereotypic response to different types of injuries and a critical upstream event of astrocytic release of inflammatory chemokines.
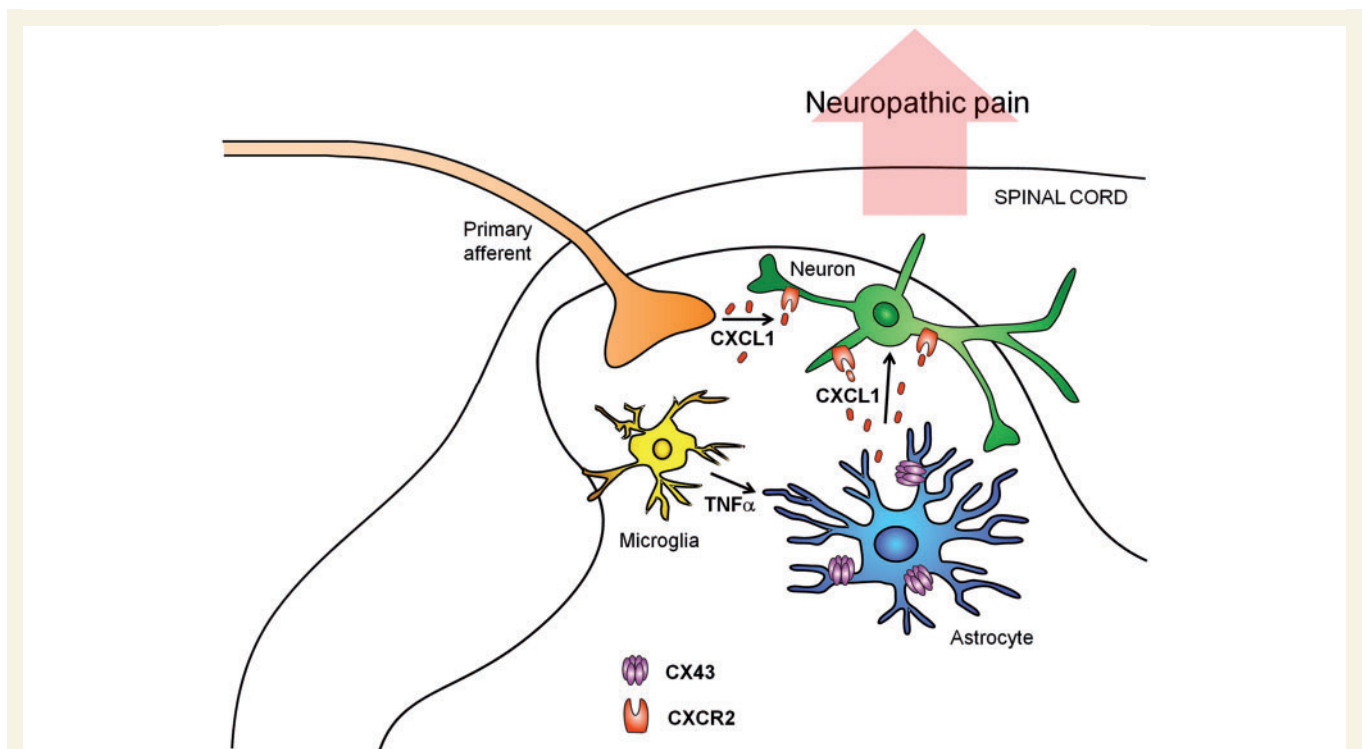
Figure 8 Schematic of working hypothesis for astrocytic Cx43-mediated late-phase neuropathic pain. CCI induces a persistent upregulation of Cx43 in spinal cord astrocytes. Cx43 expression and activity is also upregulated by TNF-α, secreted from microglia. Upregulation of Cx43 hemichannel activities results in CXCL1 release. Astrocytic CXCL1 secretion activates CXCR2 on neurons (central terminals of primary sensory neurons and spinal cord neurons), leading to enhanced excitatory synaptic transmission in nociceptive neurons (e.g. lamina IIo excitatory interneurons) and sustained neuropathic pain in the late-phase. Additionally, CXCL1 can also be secreted from intact or injured primary afferents in the spinal cord especially in the early phase of CCI.

Supplementary material

Supplementary material is available at *Brain* online.

References

Anand P, Shenoy R, Palmer JE, Baines AJ, Lai RY, Robertson J, et al. Clinical trial of the p38 MAP kinase inhibitor dilmapimod in neuropathic pain following nerve injury. Eur J Pain 2011; 15: 1040–8.

Basbaum AI, Bautista DM, Scherrer G, Julius D. Cellular and molecular mechanisms of pain. Cell 2009; 139: 267–84.

Bennett GJ, Xie YK. A peripheral mononeuropathy in rat that produces disorders of pain sensation like those seen in man. Pain 1988; 33: 87–107.

Bennett MV, Garre JM, Orellana JA, Bukauskas FF, Nedergaard M, Saez JC. Connexin and pannexin hemichannels in inflammatory responses of glia and neurons. Brain Res 2012; 1487: 3–15.

Berta T, Park CK, Xu ZZ, Xie RG, Liu T, Lü N. Extracellular caspase-6 drives murine inflammatory pain via microglial TNF-α secretion. J Clin Invest 2014; 124: 1173–86.

Chekeni FB, Elliott MR, Sandilos JK, Walk SF, Kinchen JM, Lazarowski ER, et al. Pannexin 1 channels mediate 'find-me' signal release and membrane permeability during apoptosis. Nature 2010; 467: 863–7.

Chen MJ, Kress B, Han X, Moll K, Peng W, Ji RR, et al. Astrocytic CX43 hemichannels and gap junctions play a crucial role in development of chronic neuropathic pain following spinal cord injury. Glia 2012; 60: 1660–70.

Chiang CY, Sessle BJ, Dostrovsky JO. Role of astrocytes in pain. Neurochem Res 2012; 37: 2419–2431.

Clark AK, Yip PK, Grist J, Gentry C, Staniland AA, Marchand F, et al. Inhibition of spinal microglial cathepsin S for the reversal of neuropathic pain. Proc Natl Acad Sci USA 2007; 104: 10655–60.

Contreras JE, Sánchez HA, Eugenin EA, Speidel D, Theis M, Willecke K, et al. Metabolic inhibition induces opening of unapposed connexin 43 gap junction hemichannels and reduces gap junctional communication in cortical astrocytes in culture. Proc Natl Acad Sci USA 2002; 99: 495–500.

Costigan M, Scholz J, Woolf CJ. Neuropathic pain: a maladaptive response of the nervous system to damage. Annu Rev Neurosci 2009; 32: 1–32.

Cotrina ML, Lin JH, Lopez-Garcia JC, Naus CC, Nedergaard M. ATP-mediated glia signaling. J Neurosci 2000; 20: 2835–44.

Cronin M, Anderson PN, Cook JE, Green CR, Becker DL. Blocking connexin43 expression reduces inflammation and improves functional recovery after spinal cord injury. Mol Cell Neurosci 2008; 39: 152–60.

Dixon WJ. Efficient analysis of experimental observations. Annu Rev Pharmacol Toxicol 1980; 20: 441–62.

Gao YJ, Ji RR. Chemokines, neuronal-glial interactions, and central processing of neuropathic pain. Pharmacol Ther 2010a; 126: 56–68.

Gao YJ, Ji RR. Targeting astrocyte signaling for chronic pain. Neurotherapeutics 2010b; 7: 482–93.

Gao YJ, Zhang L, Ji RR. Spinal injection of TNF-α-activated sstrocytes produces persistent pain symptom mechanical allodynia by releasing Monocyte Chemoattractant Protein-1. Glia 2010c; 58: 1871–80.

Gao YJ, Zhang L, Samad OA, Suter MR, Yasuhiko K, Xu ZZ, et al. JNK-induced MCP-1 production in spinal cord astrocytes contributes to central sensitization and neuropathic pain. J Neurosci 2009; 29: 4096–108.

Garré JM, Retamal MA, Cassina P, Barbeito L, Bukauskas FF, Sáez JC, et al. FGF-1 induces ATP release from spinal astrocytes in culture and opens pannexin and connexin hemichannels. Proc Natl Acad Sci USA 2010; 107: 22659–64.

Gold MS, Gebhart GF. Nociceptor sensitization in pain pathogenesis. Nat Med 2010; 16: 1248–57.

Guo W, Wang H, Watanabe M, Shimizu K, Zou S, LaGraize SC, et al. Glial-cytokine-neuronal interactions underlying the mechanisms of persistent pain. J Neurosci 2007; 27: 6006–18.

Horuk R, Martin AW, Wang Z, Schweitzer L, Gerassimides A, Guo H, et al. Expression of chemokine receptors by subsets of neurons in the central nervous system. J Immunol 1997; 158: 2882–90.

Huang C, Han X, Li X, Lam E, Peng W, Lou N, et al. Critical role of connexin 43 in secondary expansion of traumatic spinal cord injury. J Neurosci 2012; 32: 3333–8.

Hucho T, Levine JD. Signaling pathways in sensitization: toward a nociceptor cell biology. Neuron 2007; 55: 365–76.

Iacobas DA, Iacobas S, Urban-Maldonado M, Scemes E, Spray DC. Similar transcriptomic alterations in Cx43 knockdown and knockout astrocytes. Cell Commun Adhes 2008; 15: 195–206.

Imai S, Ikegami D, Yamashita A, Shimizu T, Narita M, et al. Epigenetic transcriptional activation of monocyte chemotactic protein 3 contributes to long-lasting neuropathic pain. Brain 2013; 136: 828–43.

Jensen MP, Chodroff MJ, Dworkin RH. The impact of neuropathic pain on health-related quality of life: review and implications. Neurology 2007; 68: 1178–82.

Ji RR, Berta T, Nedergaard M. Glia and pain: is chronic pain a gliopathy? Pain 2013; 154: S10–S28.

Ji RR, Kohno T, Moore KA, Woolf CJ. Central sensitization and LTP: do pain and memory share similar mechanisms? Trends Neurosci 2003; 26: 696–705.

Ji RR, Suter MR. p38 MAPK, microglial signaling, and neuropathic pain. Mol Pain 2007; 3: 33.

Jin SX, Zhuang ZY, Woolf CJ, Ji RR. p38 mitogen-activated protein kinase is activated after a spinal nerve ligation in spinal cord microglia and dorsal root ganglion neurons and contributes to the generation of neuropathic pain. J Neurosci 2003; 23: 4017–22.

Kalliomaki J, Attal N, Jonzon B, Bach FW, Huizar K, Ratcliffe S, et al. A randomized, double-blind, placebo-controlled trial of a chemokine receptor 2 (CCR2) antagonist in posttraumatic neuralgia. Pain 2013; 154: 761–7.

Kang J, Kang N, Lovatt D, Torres A, Zhao Z, Lin J, et al. Connexin 43 hemichannels are permeable to ATP. J Neurosci 2008; 28: 4702–11.

Katsura H, Obata K, Mizushima T, Sakurai J, Kobayashi K, Yamanaka H, et al. Activation of Src-family kinases in spinal microglia contributes to mechanical hypersensitivity after nerve injury. J Neurosci 2006; 26: 8680–90.

Kawasaki Y, Xu ZZ, Wang X, Park JY, Zhuang ZY, Tan PH, et al. Distinct roles of matrix metalloproteases in the early- and late-phase development of neuropathic pain. Nat Med 2008; 14: 331–6.

Kimelberg HK, Nedergaard M. Functions of astrocytes and their potential as therapeutic targets. Neurotherapeutics 2010; 7: 338–53.

Kobayashi K, Takahashi E, Miyagawa Y, Yamanaka H, Noguchi K. Induction of the P2X7 receptor in spinal microglia in a neuropathic pain model. Neurosci Lett 2011; 504: 57–61.

Kobayashi K, Yamanaka H, Fukuoka T, Dai Y, Obata K, Noguchi K. P2Y12 receptor upregulation in activated microglia is a gateway of p38 signaling and neuropathic pain. J Neurosci 2008; 28: 2892–902.

Kuner R. Central mechanisms of pathological pain. Nat Med 2010; 16: 1258–66.

Landry RP, Jacobs VL, Romero-Sandoval EA, DeLeo JA. Propentofylline, a CNS glial modulator does not decrease pain in post-herpetic neuralgia patients: *in vitro* evidence for differential responses in human and rodent microglia and macrophages. Exp Neurol 2012; 234: 340–50.

Manjavachi MN, Costa R, Quintão NL, Calixto JB. The role of keratinocyte-derived chemokine (KC) on hyperalgesia caused by peripheral nerve injury in mice. Neuropharmacology 2014; 79: 17–27.

Mei XP, Xu H, Xie C, Ren J, Zhou Y, Zhang H, et al. Post-injury administration of minocycline: an effective treatment for nerve-injury induced neuropathic pain. Neurosci Res 2011; 70: 305–12.

Nedergaard M, Verkhratsky A. Artifact versus reality–how astrocytes contribute to synaptic events. Glia 2012; 60: 1013–23.

Nguyen D, Stangel M. Expression of the chemokine receptors CXCR1 and CXCR2 in rat oligodendroglial cells. Brain Res Dev Brain Res 2001; 128: 77–81.

Ohara PT, Vit JP, Bhargava A, Jasmin L. Evidence for a role of connexin 43 in trigeminal pain using RNA interference *in vivo*. J Neurophysiol 2008; 100: 3064–73.

Ostenfeld T, Krishen A, Lai RY, Bullman J, Baines AJ, Green J, et al. Analgesic efficacy and safety of the novel p38 MAP kinase inhibitor, losmapimod, in patients with neuropathic pain following peripheral nerve injury: a double-blind, placebo-controlled study. Eur J Pain 2013; 17: 844–57.

Park CK, Lu N, Xu ZZ, Liu T, Serhan CN, Ji RR. Resolving TRPV1- and TNF-α-mediated spinal cord synaptic plasticity and inflammatory pain with neuroprotectin D1. J Neurosci 2011; 31: 15072–85.

Pelegrin P, Surprenant A. Pannexin-1 couples to maitotoxin- and nigericin-induced interleukin-1beta release through a dye uptake-independent pathway. J Biol Chem 2007; 282: 2386–94.

Raghavendra V, Tanga F, DeLeo JA. Inhibition of microglial activation attenuates the development but not existing hypersensitivity in a rat model of neuropathy. J Pharmacol Exp Ther 2003; 306: 624–30.

Rami A, Volkmann T, Winckler J. Effective reduction of neuronal death by inhibiting gap junctional intercellular communication in a rodent model of global transient cerebral ischemia. Exp Neurol 2001; 170: 297–304.

Ren K, Dubner R. Interactions between the immune and nervous systems in pain. Nat Med 2010; 16: 1267–76.

Retamal MA, Froger N, Palacios-Prado N, Ezan P, Saez PJ, Saez JC, et al. Cx43 hemichannels and gap junction channels in astrocytes are regulated oppositely by proinflammatory cytokines released from activated microglia. J Neurosci 2007; 27: 13781–92.

Saez JC, Retamal MA, Basilio D, Bukauskas FF, Bennett MV. Connexin-based gap junction hemichannels: gating mechanisms. Biochim Biophys Acta 2005; 1711: 215–24.

Schajnovitz A, Itkin T, D'Uva G, Kalinkovich A, Golan K, Ludin A, et al. CXCL12 secretion by bone marrow stromal cells is dependent on cell contact and mediated by connexin-43 and connexin-45 gap junctions. Nat Immunol 2011; 12: 391–8.

Shi Y, Gelman BB, Lisinicchia JG, Tang SJ. Chronic-pain-associated astrocytic reaction in the spinal cord dorsal horn of human immunodeficiency virus-infected patients. J Neurosci 2012; 32: 10833–40.

Spataro LE, Sloane EM, Milligan ED, Wieseler-Frank J, Schoeniger D, Jekich BM, et al. Spinal gap junctions: potential involvement in pain facilitation. J Pain 2004; 5: 392–405.

Stout CE, Costantin JL, Naus CC, Charles AC. Intercellular calcium signaling in astrocytes via ATP release through connexin hemichannels. J Biol Chem 2002; 277: 10482–8.

Todd AJ. Neuronal circuitry for pain processing in the dorsal horn. Nat Rev Neurosci 2010; 11: 823–36.

Tozaki-Saitoh H, Tsuda M, Miyata H, Ueda K, Kohsaka S, Inoue K. P2Y12 receptors in spinal microglia are required for neuropathic pain after peripheral nerve injury. J Neurosci 2008; 28: 4949–56.

Tsuda M, Inoue K, Salter MW. Neuropathic pain and spinal microglia: a big problem from molecules in "small" glia. Trends Neurosci 2005; 28: 101–7.

Tsuda M, Kohro Y, Yano T, Tsujikawa T, Kitano J, Tozaki-Saitoh H, et al. JAK-STAT3 pathway regulates spinal astrocyte proliferation and neuropathic pain maintenance in rats. Brain 2011; 134: 1127–39.

Tsuda M, Shigemoto-Mogami Y, Koizumi S, Mizokoshi A, Kohsaka S, Salter MW, et al. P2X4 receptors induced in spinal microglia gate tactile allodynia after nerve injury. Nature 2003; 424: 778–83.

Valles A, Grijpink-Ongering L, de Bree FM, Tuinstra T, Ronken E. Differential regulation of the CXCR2 chemokine network in rat brain trauma: implications for neuroimmune interactions and neuronal survival. Neurobiol Dis 2006; 22: 312–22.

van Hecke O, Austin SK, Khan RA, Smith BH, Torrance N. Neuropathic pain in the general population: A systematic review of epidemiological studies. Pain 2013; 155: 654–62.

Vanelderen P, Rouwette T, Kozicz T, Heylen R, Van Zundert J, Roubos EW, et al. Effects of chronic administration of amitriptyline, gabapentin and minocycline on spinal brain-derived neurotrophic factor expression and neuropathic pain behavior in a rat chronic constriction injury model. Reg Anesth Pain Med 2013; 38: 124–30.

Wang H, Cao Y, Chiang CY, Dostrovsky JO, Sessle BJ. The gap junction blocker carbenoxolone attenuates nociceptive behavior and medullary dorsal horn central sensitization induced by partial infraorbital nerve transection in rats. Pain 2014; 155: 429–35.

Wang N, De Bock M, Antoons G, Gadicherla AK, Bol M, Decrock E, et al. Connexin mimetic peptides inhibit Cx43 hemichannel opening triggered by voltage and intracellular Ca2 + elevation. Basic Res Cardiol 2012; 107: 304.

Watkins LR, Maier SF. Immune regulation of central nervous system functions: from sickness responses to pathological pain. J Intern Med 2005; 257: 139–55.

Wen YR, Tan PH, Cheng JK, Liu YC, Ji RR. Microglia: a promising target for treating neuropathic and postoperative pain, and morphine tolerance. J Formos Med Assoc 2011; 110: 487–94.

White FA, Jung H, Miller RJ. Chemokines and the pathophysiology of neuropathic pain. Proc Natl Acad Sci USA 2007; 104: 20151–8.

White JR, Lee JM, Young PR, Hertzberg RP, Jurewicz AJ, Chaikin MA, et al. Identification of a potent, selective non-peptide CXCR2 antagonist that inhibits interleukin-8-induced neutrophil migration. J Biol Chem 1998; 273: 10095–8.

Wu XF, Liu WT, Liu YP, Huang ZJ, Zhang YK, Song XJ. Reopening of ATP-sensitive potassium channels reduces neuropathic pain and regulates astroglial gap junctions in the rat spinal cord. Pain 2011; 152: 2605–15.

Xu ZZ, Liu XJ, Berta T, Park CK, Lu N, Serhan CN, et al. Neuroprotectin/Protectin D1 protects neuropathic pain in mice after nerve trauma. Ann Neurol 2013; 74: 490–5.

Ye ZC, Wyeth MS, Baltan-Tekkok S, Ransom BR. Functional hemichannels in astrocytes: a novel mechanism of glutamate release. J Neurosci 2003; 23: 3588–96.

Yoon SY, Robinson CR, Zhang H, Dougherty PM. Spinal astrocyte gap junctions contribute to oxaliplatin-induced mechanical hypersensitivity. J Pain 2013; 14: 205–14.

Zhang J, De Koninck Y. Spatial and temporal relationship between monocyte chemoattractant protein-1 expression and spinal glial activation following peripheral nerve injury. J Neurochem 2006; 97: 772–83.

Zhang J, Shi XQ, Echeverry S, Mogil JS, De Koninck Y, Rivest S. Expression of CCR2 in both resident and bone marrow-derived microglia plays a critical role in neuropathic pain. J Neurosci 2007; 27: 12396–406.

Zhang ZJ, Cao DL, Zhang X, Ji RR, Gao YJ. Chemokine contribution to neuropathic pain: respective induction of CXCL1 and CXCR2 in spinal cord astrocytes and neurons. Pain 2013; 154: 2185–97.

Zhuang ZY, Wen YR, Zhang DR, Borsello T, Bonny C, Strichartz GR, et al. A peptide c-Jun N-terminal kinase (JNK) inhibitor blocks mechanical allodynia after spinal nerve ligation: respective roles of JNK activation in primary sensory neurons and spinal astrocytes for neuropathic pain development and maintenance. J Neurosci 2006; 26: 3551–60.